ISSN 0015-4628, Fluid Dynamics, 2023, Vol. 58, No. 5, pp. 864–872. © The Author(s), 2023. This article is an open access publication.
Russian Text © The Author(s), 2023, published in Izvestiya RAN. Mekhanika Zhidkosti i Gaza, 2023, No. 5, pp. 37–46.

Self-Similar Flows with a Shock Wave Advancing toward the Center or Axis of Symmetry

Kh. F. Valiev[a] and A. N. Kraiko[a,*]

[a] *Baranov Central Institute of Aviation Motors (CIAM), Moscow, 111116 Russia*

**e-mail: akraiko@ciam.ru*

Received June 4, 2023; revised June 6, 2023; accepted June 6, 2023

Abstract—We study one-dimensional flows of an ideal (inviscid and non-heat-conducting) perfect gas with an adiabatic exponent γ behind a shock wave moving toward the center ($\nu = 3$) or axis ($\nu = 2$) of symmetry in a cold gas at rest. Flows with a reflected shock wave and flows terminating with simultaneous arrival of a shock wave and a piston, which has compressed the gas into a point or line, to the center of symmetry are admitted.

Keywords: center (axis) of symmetry, pistons and shock waves, C^--envelope of characteristics, non-self-sinilar shock waves, self-sinilar flows with compression into a point (line)

DOI: 10.1134/S001546282370009X

The first self-similar solution with a reflected shock wave was found by Guderley. In his solution the self-similarity exponent $n = n_*(\nu, \gamma) < 1$ is determined from the condition that the flow under consideration does exist. At $n = n_*(\nu, \gamma)$ there can also exist self-similar solutions with a piston expanding from the center of symmetry after the arrival of a convergent shock wave to this point; these solutions have not been considered earlier. The attention to the flows with $n \neq n_*(\nu, \gamma)$ was attracted in 2015–2017 by V. Kuropatenko with his colleagues. An analysis of these flows made below shows that the flows with a reflected shock wave constructed for $n > n_*(\nu, \gamma)$ are self-similar only in a curvilinear triangle in the coordinate-time plane. One of its sides is a segment of the trajectory of a self-similar shock wave that has not arrived at the center of symmetry. At $n < n_*(\nu, \gamma)$ these solutions become the completely self-similar flows of gas compression to a point constructed by Kuropatenko.

1. SELF-SIMILAR SOLUTIONS ON THE TIME-DEPENDENT SHOCK WAVE REFLECTION FROM AN AXIS OF CENTER OF SYMMETRY

In 1942 Guderley [1] (see also [2, 3]) solved the problem of the reflection of a shock wave (SW) from the axis or center of symmetry (below, from the "center of symmetry" (CS)). As a SW approaches the CS, its intensity increases without bound. It is possible that precisely for this reason the solutions searched in [1] were self-similar solutions with a strong SW *IS* moving throughout a cold gas at rest at a velocity $D = D(t) < 0$ with the time t reference point at the moment of SW *IS* arrival to the CS. For a perfect gas its radial velocity u, speed of sound a, density ρ, and pressure p behind a strong SW are as follows [2–5]:

$$u = \frac{2}{\gamma+1} D, \quad a = -\frac{\sqrt{2\gamma(\gamma-1)}}{\gamma+1} D, \quad \rho = \frac{\gamma+1}{\gamma-1}\rho_0, \quad p = \frac{2}{\gamma+1}\rho_0 D^2. \tag{1.1}$$

At a radial coordinate r the flow parameters can be represented in one of two equivalent forms with the self-similar variable ξ or τ

$$\xi = Cr \times \begin{cases} (-t)^{-n}, & t \le 0, \\ t^{-n}, & t > 0; \end{cases} \qquad \tau = \frac{Ct}{r^k}, \quad k = \frac{1}{n},$$
$$u = n\frac{r}{t}U, \quad a = n\frac{r}{t}A, \quad \rho = \rho_0 R, \quad p = \rho_0 n^2 \frac{r^2}{t^2} P, \quad P = \frac{R}{\gamma} A^2. \tag{1.2}$$

In Guderley's solution the exponent n is to be determined, U, A, and R are functions of ξ or τ, and the constant C is arbitrary. Guderley worked with the coordinate ξ, which is finite on the SW *IS*, infinite at the r axis, and zero at the semi-axis $t > 0$. The variable τ, the same for all t, with $C > 0$ increases monotonically from a negative value on the SW *IS* to zero at the r axis and to infinity at the semi-axis $t > 0$.

The ordinary differential equations obtained by means of substituting the representations (1.2) with the variable τ into the equations governing the time-dependent flows of an ideal perfect gas having only one nonzero r-component of the velocity vector u reduce to the system of equations

$$\frac{dA}{dU} = \frac{Af_2}{2(1-U)f_1}, \quad \frac{d\tau}{dU} = \gamma k\frac{\tau f}{f_1}, \quad \frac{d\ln R}{dU} = \frac{f_3}{(1-U)f_1},$$
$$f = (1-U)^2 - A^2, \quad f_1 = \gamma(1-U)(k-U)U + (2k-2-\nu\gamma U)A^2, \tag{1.3}$$
$$f_2 = \gamma[2(k-U) - \nu(\gamma-1)U]f + (\gamma-1)f_1, \quad f_3 = f_1 - \nu\gamma Uf.$$

The substitution of the same representations into relations (1.1), in which, due to these representations, $D = r_{IS}/(kt) = nr_{IS}/t$, yields

$$U_{IS} \equiv U(\tau_{IS}) = \frac{2}{\gamma+1}, \quad A_{IS} = -\frac{\sqrt{2\gamma(\gamma-1)}}{\gamma+1}, \quad R_{IS} = \frac{\gamma+1}{\gamma-1}. \tag{1.4}$$

The constant C, which does not enter in Eqs. (1.3) and representations (1.4), can be chosen such that the quantity τ_{IS} is equal to any number, for example, -1. The representation of the SW IS as a power-law curve $r^{k>1} = -Ct$, that arrives to the CS at $t = 0$, does not ensure the existence of such a flow. An analysis of the integral curves and singular points of the first equation (1.3) can help to understand this fact. At the r axis and $r > 0$ the variable $\tau = 0$, while u and a are finite. According to Eq. (1.2), this is possible only at $U(0) = A(0) = 0$. For this reason, for any $k > 1$ the integral curves of solutions containing the r axis or its finite interval originating at a point on *IS* with U and A from Eq. (1.4) must arrive at the origin $A = U = 0$ of the *UA* plane. However, the point on *IS* lies beneath the "sonic" line $A = U - 1$ presented by dashes in Fig. 1. At this line the function f from the second equation (1.3) is zero, while the integral curve proceeding from point IS must intersect it. For an arbitrary k the function $f_1 \neq 0$ at the point of intersection between the integral curve and the sonic line and the function τ has a local maximum $\tau = \tau_{0*}$ at this point rather than increases monotonically; the occurrence of this maximum excludes the continuation of the solution toward the region, where $\tau > \tau_{0*}$. In Fig. 1 and in what follows the arrows on the integral curves indicate the direction of the growth of the variable τ, while on the red curve the function $f_1(U, A)$ is zero.

Any point on the line $A = U - 1$ in the *UA* plane is associated with a curve with $dr/dt = u - a$ in the *rt* plane, as in the case of the C$^-$-characteristics. However, these curves are the envelopes of the C$^-$-characteristics rather than the C$^-$-characteristics themselves, since the compability conditions for C$^-$-characteristics are not fulfilled on these curves at $f_1 \neq 0$. The envelope becomes a C$^-$-characteristic, if two conditions are fulfilled at the intersection point, namely, $f = 0$ and $f_1 = 0$. Their consequence, that is, the equality $f_2 = 0$, makes the intersection point a singular point (saddle *SP* or node *NP*) of the first equation (1.3). The passage through the sonic line becomes possible along the integral curve coinciding with one of separatrices of the saddle or with the basic appendix of a node, while the choice $n = n_*(\nu,\gamma)$ makes it possible to join the singular point with the point *IS* by means of the integral curve. For $\nu = 3$ and $\gamma = 5/3$ precisely this situation with the saddle *SP* and $n_* = 0.68838$ is presented in Fig. 1. The origin $A = U = 0$ is a node of the first equation (1.3) with the bald integral curve that interested the sonic line and arrived at it. For $\nu = 2$ and 3 and several values of γ the quantities $n_* = n_*(\nu,\gamma)$ are presented in Table 1.

At $k = k_* = 1/n_* > 1$ the pressure p and the entropy function $S = \gamma p/\rho^\gamma$ behind the SW *IS* are infinite at the moment of its arrival at CS. With any increase in the reflected SW *RS* the function S remains infinite in the CS (at $r = 0$ and $t > 0$). However, at $p = \infty$ the gas expands instantaneously to a finite pressure and zero density, which, having conserved $S = \infty$, turn the speed of sound to infinity, $a = (\gamma p/\rho)^{1/2} = n_*(r/t)A = \infty$, at the semiaxis $t > 0$. Thus, $A(\tau = \infty) = \infty$ and transition from A to the variable $\delta = 1/A$ lead to the equation

$$\frac{d\delta}{dU} = \frac{\delta f_2}{2(U-1)f_1}, \quad \frac{d\tau}{dU} = \gamma k_*\frac{\tau f}{f_1},$$
$$f = (1-U)^2\delta^2 - 1, \quad f_1 = \gamma(1-U)(k_*-U)U\delta^2 + 2(k_*-1) - \nu\gamma U, \tag{1.5}$$
$$f_2 = (\gamma-1)f_1 + \gamma[2(k_*-U) - \nu(\gamma-1)U]f.$$

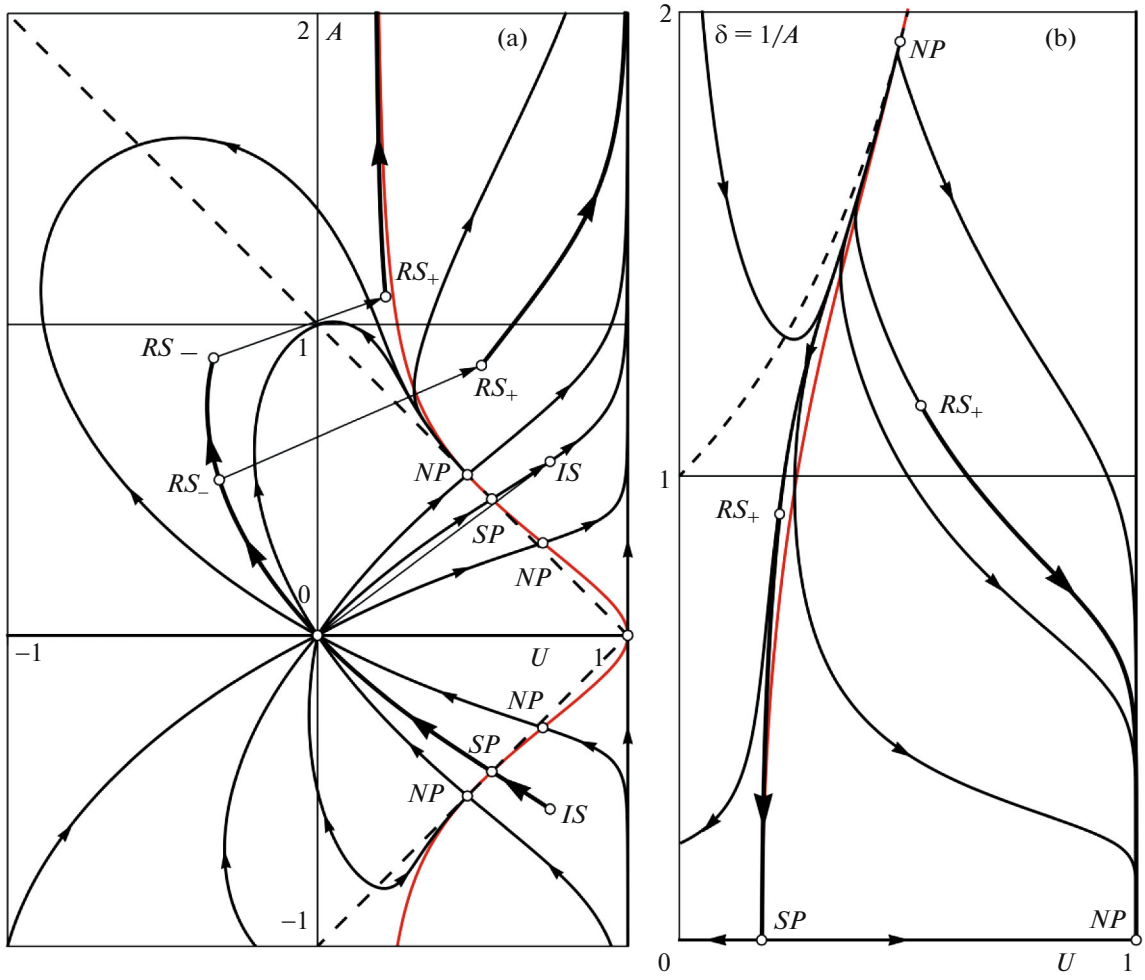

Fig. 1. Integral curves, singular points, and "sonic" lines: $f = 0$ and SW *RS* (upper arrow) in Guderley's solution for $\nu = 3$, $\gamma = 5/3$, and $n_* = 0.68838$.

The U axis, at which $\delta = 0$, is the integral curve of the first equation (1.5). The other integral curves can arrive at this axis only through its singular points $\delta = 0$, $U = 1$ and $\delta = 0$, $U = 2(k_* - 1)/(\nu\gamma)$. In Fig. 1b the former point is a node and the latter one is a saddle. In view of the second equation (1.5), the variable τ is finite at the node, whereas at the saddle $\tau = \infty$. For this reason, a portion of the unknown integral curve is a segment of the saddle separatrix. The solution arrives jumpwise from point RS_- at point RS_+ on the separatrix (upper arrow in Fig. 1a), and for U_+ and A_+ behind the reflected SW *RS* the following equations hold true [5]

$$U_+ = 1 - \frac{2A_-^2 + (\gamma - 1)(1 - U_-)^2}{(\gamma + 1)(1 - U_-)},$$
$$A_+ = \frac{\sqrt{2(\gamma - 1)[\gamma(1 - U_-)^4 - A_-^4] + (6\gamma - \gamma^2 - 1)A_-^2(1 - U_-)^2}}{(\gamma + 1)(1 - U_-)}. \tag{1.6}$$

When constructing the solution the point RS_- with U_- and A_- on the integral curve that came from point *IS* is so chosen that, in accordance with Eqs. (1.6), the point RS_+ arrives at the separatrix of the saddle of the first equation (1.5) that comes from above in Fig. 1b.

The fourth quadrant of Fig. 1a and a portion of the *rt*-diagram corresponding to the bold segment of the integral curve connecting point *IS* with the origin $U = A = 0$ are presented in Fig. 2 on a larger scale. In Fig. 2b the left (right) bold curve that proceeds from point *1* is the SW *IS* (piston trajectory), while the

Table 1. Exponents $n_0 = n_0(\nu, \gamma)$ and $n_* = n_*(\nu, \gamma)$

ν	γ	n_0	n_*
2	3	0.33333	0.77567
2	5/3	0.60000	0.81562
2	7/5	0.71429	0.83532
2	4/3	0.75000	0.84226
2	6/5	0.83333	0.86116
3	3	0.25000	0.63641
3	5/3	0.50000	0.68838
3	7/5	0.62500	0.71717
3	4/3	0.66667	0.72769
3	6/5	0.76923	0.75714

segments connecting them are C^--characteristics. One of these segments that connects point 0^- with the origin is a C^--characteristic corresponding to the saddle *SP* on the sonic line in Fig. 2a. On the semiaxis $t > 0$, which is not presented on the *rt*-diagram, the gas velocity $u = n_* rU/t = 0$, as it must be in the CS.

Although many researchers studied the Guderley solution, the most complete and important results have been obtained by the authors of this paper [5–8]. It is true that, starting from Guderley all the authors took no notice of the self-similar solutions with a piston that started its expansion from the CS at the moment of the arrival of the SW *IS* from the Guderley solution. We will fill this gap.

Letting $A_- = U_- = 0$ in Eq. (1.6) we arrive at the following values

$$U_+ = U_{IS} = \frac{2}{\gamma+1}, \quad A_+ = A_{IS} = \frac{\sqrt{2\gamma(\gamma-1)}}{\gamma+1} \tag{1.7}$$

behind the strong SW moving from the CS; in Fig. 1a it is shown by an arrow between the origin and the upper point *IS*. The SW with U_{IS} and A_{IS} from Eq. (1.7) is the most intense from the family of SWs, whose values of U_- and A_- correspond to the points on the segment of the bold integral curve from the second quadrant in Fig. 1a. The integral curves along which the values of *U* and *A* vary from the SW to the piston, are terminated at the node $U = 1$, $\delta = 0$ in Fig. 1b. Figure 3 presents the *rt*-diagram for one of these self-

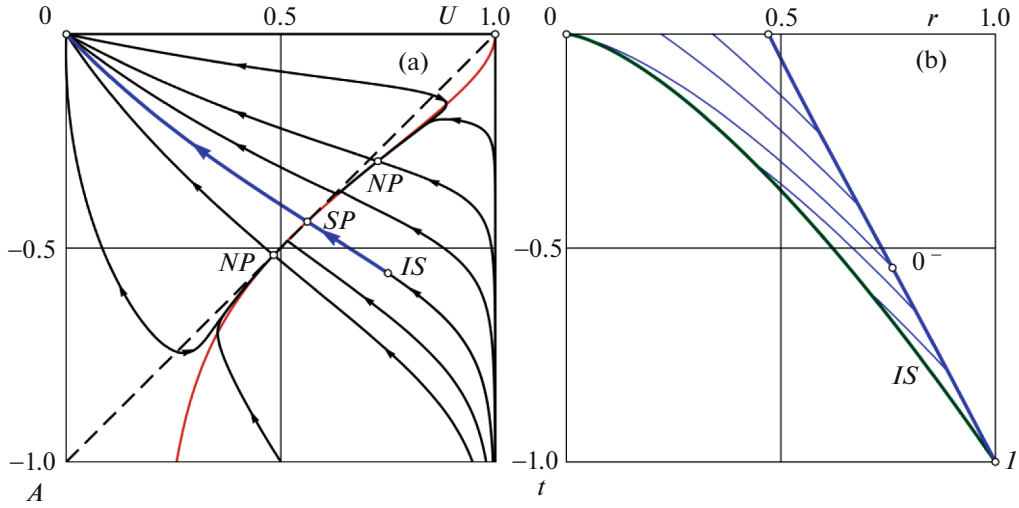

Fig. 2. Quadrant IV in the *UA* plane (a) and a part of the *rt*-diagram (b) of Guderley's solution with SW reflection from the CS for $\nu = 3$, $\gamma = 5/3$, and $n_* = 0.68838$.

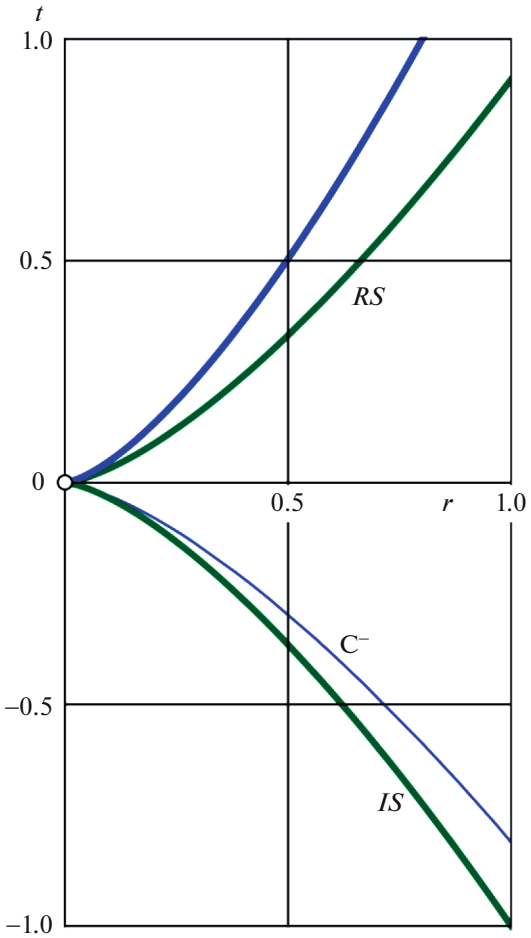

Fig. 3. *rt*-Diagram of the self-similar flow with a piston that began to expand from the CS with arrival the SW *IS* to it for $\nu = 3$, $\gamma = 5/3$, and $n = n_* = 0.68838$.

similar flows with the former values of ν, γ, and n_* but with $U_- \approx -0.32$ and $A_- = 0.50$ and one more arrow in Fig. 1a. The left upper curve in Fig. 3 is the trajectory of a piston expanding from CS at $t \geq 0$.

2. KUROPATENKO's SELF-SIMILAR SOLUTIONS WITH A SHOCK WAVE PROPAGATING TOWARD THE AXIS OR CENTER OF SYMMETRY

We will continue an investigation of flows with a SW propagating toward a CS in the case of the self-similarity exponent $1 < k \neq k_* = 1/n_*$. They were studied by Kuropatenko with his colleagues [9–13] who used, together with r, the Lagrangian mass variable m, where the self-similarity index is $l = \nu n$ rather than n itself. Then it was accepted that the flows under consideration with a strong SW in motion in a cold gas at rest are generated by a piston traveling from point *1* with $r = r_1$, $m = m_1$, and $t = t_1 < 0$ toward the CS. In this case, the gas density ρ and velocity u, as well as the coordinate r, were sought using the separation of variables and invoking conditions (1.1) valid in the case of strong SWs, in the form:

$$\xi = \frac{m}{m_1}\left(\frac{t_1}{t}\right)^l, \quad \rho = \frac{\gamma+1}{\gamma-1}\rho_0\delta(\xi), \quad r^{\nu-1}u = r_1^{\nu-1}u_1\left(\frac{t}{t_1}\right)^{l-1} Z(\xi),$$
$$r^\nu = r_1^\nu\left(\frac{t}{t_1}\right)^l X(\xi), \quad \frac{1}{t_1} = \nu\frac{\gamma+1}{2lr_1}u_1, \tag{2.1}$$

$$\delta(1) = Z(1) = X(1) = 1. \tag{2.2}$$

Here, u_1 is the gas velocity behind the SW *IS* at point *1*.

Substituting conditions (2.1) in the Euler equations governing the flows under consideration in the variables t and m leads to ordinary differential equations (the primes denote the differentiation with respect to $\xi \geq 1$)

$$G\delta' = H, \quad GZ' = \frac{\gamma-1}{2\delta^2}\xi H, \quad \xi X' = X - \frac{2Z}{\gamma+1}, \quad G = \frac{\gamma\delta^{\gamma-1}X^{2-2/\nu}}{\xi^{2/l-2/\nu}} - \frac{\gamma-1}{2\delta^2}\xi^2,$$
$$H = 2\frac{(\nu-l)\delta^{\gamma}X^{2-2/\nu}}{\nu l\xi^{1+2/l-2/\nu}} - \frac{l-1}{l}Z + \frac{2(\nu-1)Z^2}{\nu(\gamma+1)X}. \tag{2.3}$$

In [9–13] the solution of the Cauchy problem for Eqs. (2.3) with the initial conditions (2.2) led to different results for n (or $l = \nu n$) greater or smaller than n_* (or $l_* = \nu n_*$). For $n > n_*$ the function G_{0*} always turned to zero at a certain $\xi_{0*} > 1$, the function H_{0*} being in the general case different from zero. The assertion of the authors of [8–12] that in this case the curve $m/m_1 = \xi_{0*}(t/t_1)^l$ arriving at the CS is a C$^-$-characteristic is erroneous. The equality $G_{0*} = 0$ means that on this curve there holds the equality $dr/dt = u - a$, that is, the C$^-$-characteristics are only tangent to it. It becomes a C$^-$-characteristic only when the equality $H_{0*} = 0$, equivalent to the compatibility condition for C$^-$characteristics, holds true on it, along with $G_{0*} = 0$. At $H_{0*} \neq 0$ it is their envelope making impossible the construction of self-similar piston trajectories at $\xi > \xi_{0*}$ and $t > t_{0*}$, which indicates also the formation at point 0_* of a non-self-similar SW represented by the third segment of the boundary which does not reach the CS of the self-similar flow region, which is triangular in the *rt* plane.

The indices $n_*(\nu, \gamma)$ found in [9–13], at which the functions G_{0*} and H_{0*} turn simultaneously to zero for all ν and γ considered, are the same as those obtained in [1, 2, 5–8]. With account for this fact, which was not anyway mentioned in [9–13], and the greater simplicity of the customary self-similar approach we will continue an analysis of solutions for $n \neq n_*$ within the framework of equations and conditions (1.2)–(1.4), assuming, following Kuropatenko, that the flows under study are produced by a piston that starts its motion toward the CS from point *1* in the *rt* plane, on the SW *IS*. In view of Eqs. (1.2) and (1.3), the following equalities hold on the piston trajectory $dr/dt = u$

$$\frac{dt}{t} = \frac{1}{1-U}\frac{d\tau}{\tau}, \quad \frac{dr}{r} = \frac{U/k}{1-U}\frac{d\tau}{\tau}. \tag{2.4}$$

According to these equalities, the variations in time and the piston tralectory coordinate at $0 < U < 1$ are analogous to the variation in the variable τ. Thus, if $|\tau_0| > 0$ at the end of an integral curve, then $|t_0| > 0$ and $r_0 > 0$, that is, the piston does not reach the CS. If, on the contrary, $\tau_0 = 0$, then $t_0 = r_0 = 0$ and these solutions describe the gas compression to a point.

The flows with $|\tau_0| > 0$ are realized, if the integral curve of the first equation (1.3) started at point *IS* arrives at point 0_* on the line $A = U - 1$ in the *UA* plane with $f_1(U_{0*}, A_{0*}) \neq 0$. The quantity $\tau_{0*} < 0$ reaches a local minimum at this point; in view of this fact, the contibuation of the self-similar solution toward the values of τ greater than τ_{0*} turns out to be impossible. As in [9–13], this situation takes place always for $1 > n > n_*(\nu, \gamma)$. The typical field of the integral curves and singular points of the first equations (1.3) in the fourth quadrant of the *UA* plane and an incomplete *rt*-diagram for this case are presented in Fig. 4.

As noted above, at $f_1 \neq 0$ the point 0_* of the integral curve arriving onto the sonic line in the *UA* plane is associated with envelope $Ct = r^k\tau_{0*}$ of the C$^-$-characteristics presented as a dashed line in the *rt*-diagram in Fig. 4b. This envelope, as the self-similar SW *IS* that has come from point *1* simulataneously with the piston along the trajectory with the equation $Ct = -r^k$, may at first glance arrive at CS. However, this will not happen, since the appearance of the envelope indicates the formation of a non-self-similar SW at the point 0_* of the piston trajectory. The SW that appeared at $t < t_S$ outdistancing the C$^-$-characteristic 0_*–S and annealing it will overtake the self-similar SW *IS* before its arrival at CS. Therefore, at $n > n_*$ the self-similar solution can be realized only in a curvilinear triangle in the *rt* plane distant from the CS and confined by the piston trajectory *1*–0_* and the segements of the self-similar SW *IS* and the non-self-similar SW that appeared at point 0_* of the piston trajectory and overtook it. In a much smaller vicinity of the CS

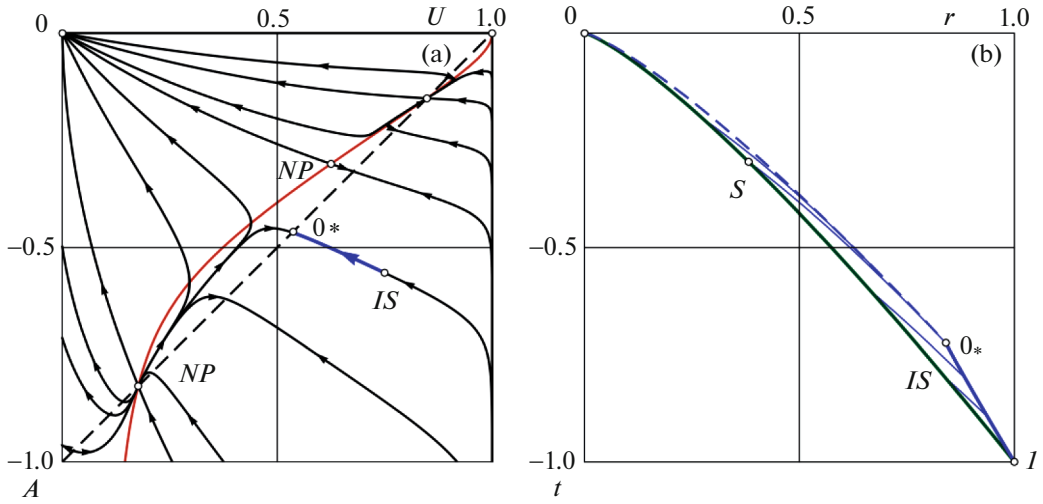

Fig. 4. *UA* plane (a) and incomplete *rt*-diagram (b) for a flow with a SW moving toward the CS for $\nu = 3$, $\gamma = 5/3$, and $n = 0.8 > n_* = 0.68838$.

the non-self-similar SW moving in the cold gas becomes the self-similar SW of Guderley's solution with $n = n_*(\nu, \gamma)$.

More interesting self-similar solutions with the SW *IS* coming to the CS and a piston compressing the gas to a point are obtained in the case of the exponents $n < n_*(\nu, \gamma)$. At $n_* > n > n_0$, where $n_0 = n_0(\nu, \gamma)$ is determined below (certain values of n_0 are given in Table 1), the solution is given by a segment of an integral curve of the first equation (1.3) with the origin at the point on *IS* with *U* and *A* from Eq. (1.4) and the end in a node beneath the sonic line from the fourth quadrant in the *UA* plane. The values of *U* and *A* at the node are determined by the equations $f_1(U, A) = 0$ and $f_2(U, A) = 0$. In accordance with these equations, the following equalities and inequalities hold true for these *n*

$$n_*(\nu,\gamma) > n > n_0 = \frac{2}{2+\nu(\gamma-1)}, \quad U = \frac{n_0}{n} < 1,$$
$$A^2 = B \equiv \frac{\gamma(1-U)(1-nU)U}{(2+\nu\gamma U)n-2} > 0, \quad A = -\sqrt{B}.$$

The quantity τ in the node turns out to be zero, thus leading, by virtue of Eqs. (2.4), to $t = 0$ and $r = 0$, that is, to a self-similar flow with a piston and a strong SW that compress the gas to a point. The above-said is illustrated in Fig. 5. The meaning of the lines and points presented in this figure is the same as in Figs. 1–4. Thus, in Fig. 5b the thin segments are the C^--characteristics coming from the piston trajectory toward the SW *IS*.

At even smaller values of the exponent *n*, $0 < n < n_0 < n_*$, it is the degenerate singular point $U = 1$ and $A = 0$ that becomes the singular point, where the integral curve of the first equation (1.3) with the origin at the point on IS with *U* and *A* from Eq. (1.4) arrives. In accordance with [14] and the calculations made by us, the integral curves that gives the solution enters to this singular point being tangent to the vertical integral line $U = 1$ and realizing, as in the case presented in Fig. 5, the self-similar solution of the shock compression of the gas to a point ($r = t = 0$). In the vicinity of this singular point we obtain

$$U \approx 1 - KA^2 < 1, \quad \tau \approx \tau_0\left[1 + \frac{\gamma K/(1-n)}{2-\gamma(\gamma-1)K}A^2\right], \quad 0 < K < \frac{2}{\gamma(\gamma-1)}$$

with the integration constant *K*.

The results of the calculations performed for two such values of *n*, are presented in Figs. 6 and 7, which are similar with Fig. 5.

3. SUMMARY

The self-similar solutions with $n = n_*$ and a piston starting its expansion from the CS, where the SW *IS* comes, and the self-similar solutions obtained at $1 > n > n_*$ in a curvilinear triangle in the *rt* plane with

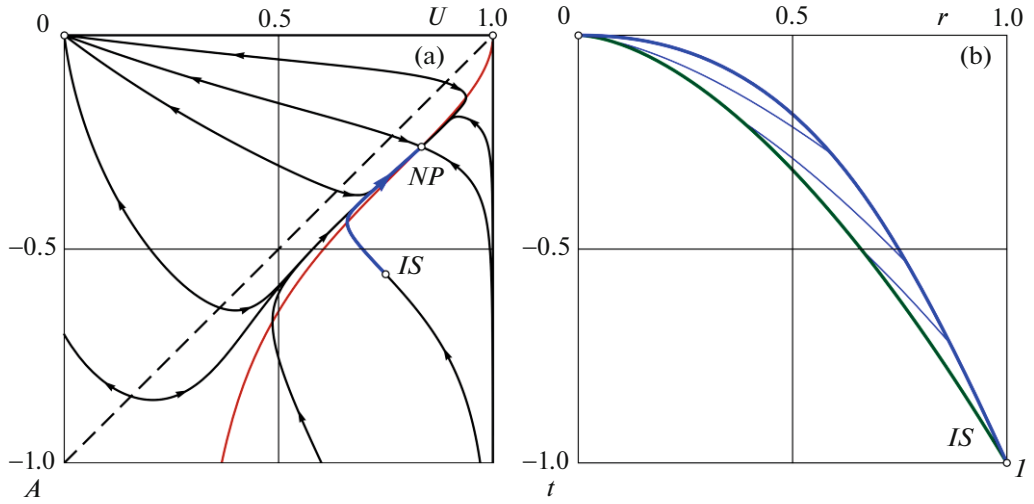

Fig. 5. *UA* plane (a) and *rt*-diagram (b) for a flow with a piston and a SW, which compress the gas to a point, for $\nu = 3$, $\gamma = 5/3$, and $n_0 = 0.5 < n = 0.6 < n_* = 0.68838$.

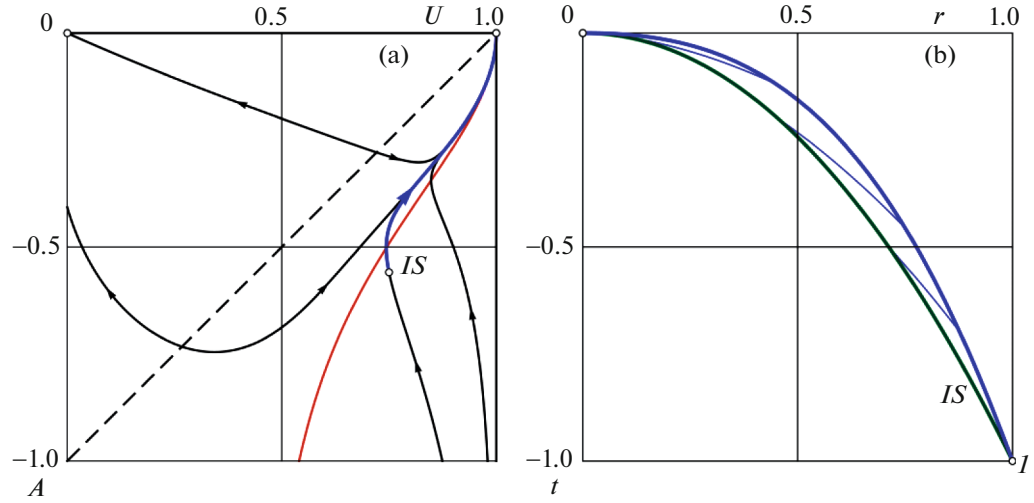

Fig. 6. *UA* plane (a) and *rt*-diagram (b) for a flow with a piston and a SW which compress the gas to a point, for $\nu = 3$, $\gamma = 5/3$, and $n = 0.49 < n_0 = 0.5 < n_* = 0.68838$.

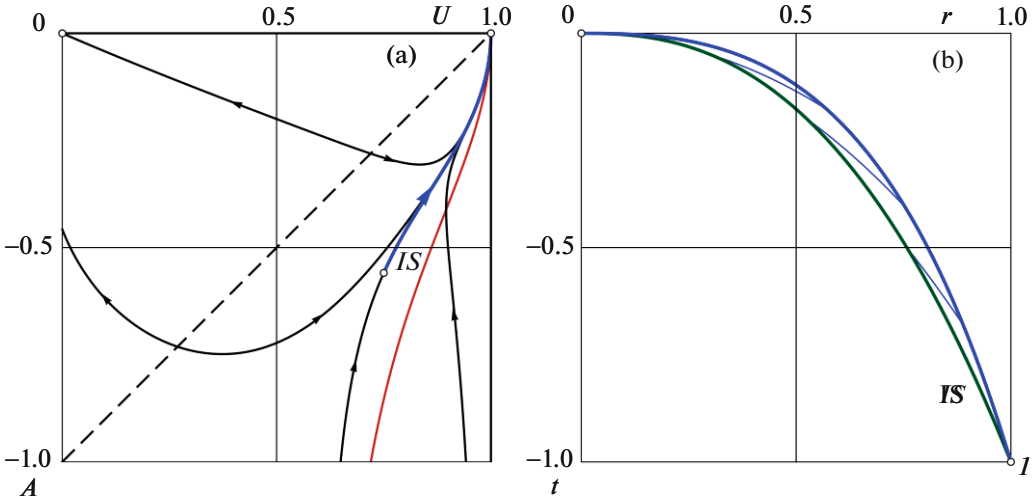

Fig. 7. *UA* plane (a) and *rt*-diagram (b) for a flow with a piston and SW, which compress the gas to a point, for $\nu = 3$, $\gamma = 5/3$, and $n = 0.4 < n_0 = 0.5 < n_* = 0.68838$.

$r > 0$ present an unterest exceptionally for the theory. The self-similar solutions of shock compression of a gas to a point, which are obtained at $n_* > n > 0$, present an interest also mainly for the theory, since in these cases the greater portion of the pistom work, and at $n_0 > n$ even its entire work, is spent for an increase in the kinetic energy of the compressed gas.

In connection with the solutions for $n \neq n_*$, the study made above, having specified certain details [9–13], demonstrates the applicability and a greater simplicity of the habitual self-similar approach with one equation (1.3) and the qualitative analysis of the integral curves in the *UA* plane, as compared with the separation of variables and the solution of the system of three equations (2.3). The main merit of Kuropatenko and his colleagues lies in the fact that they have found new self-similar solutions describing the compression of a cold gas at rest to a point.

FUNDING

The study is carried out with the financial support of the Russian Foundation for Basic Research under grant no. 20-01-00100.

CONFLICT OF INTEREST

The authors declare that they have no conflicts of interest.

REFERENCES

1. Guderley, G., Starke kugelige und zylindrische Verdichtungsstöße in der Nähe des Kugelmittelpunktes bzw. der Zylinderachse, *Luftfartforschung*, 1942, vol. 19, no. 9, pp. 302–312.
2. Brushlinskii, K.V. and Kazhdan, Ya.M., On auto-models in the solution of certain problems of gas dynamics, *Russian Math. Surveys*, 1963, vol. 18, no. 2, pp. 1–22.
3. Landau, L.D. and Lifshitz, E.M., *Fluid Mechanics*, Oxford: Pergamon, 1987.
4. Chernyi, G.G., *Gazovaya dinamika* (Gas Dynamics), Moscow: Nauka, 1988.
5. Kraiko, A.N., *Teoreticheskaya gazovaya dinamika: klassika i sovremennost'* (Theoretical Gas Dynamics: Classics and Modern), Moscow: Torus Press, 2010.
6. Kraiko, A.N. and Tillyaeva, N.I., Self-similar compression of ideal gas by a disk, cylindrical or spherical piston, *High Temperature*, 1998, vol. 36, no. 1, pp. 116–124.
7. Valiyev, K.F., The reflection of a shock wave from a centre or axis of symmetry with adiabatic exponents from 1.2 to 3, *J. Appl. Math. Mech.*, 2009, vol. 73, no. 3, pp. 281–289.
8. Valiyev, Kh.F. and Kraiko, A.N., Cylindrically and spherically symmetrical rapid intense compression of an ideal perfect gas with adiabatic exponents from 1.001 to 3, *J. Appl. Math. Mech.*, 2011, vol. 75, no. 2, pp. 218–226.
9. Kuropatenko, V.F., Shestakovskaya, E.S., and Yakimova, M.N., Dynamic compression of a cold gas sphere, *Doklady Phys.*, 2015, vol. 60, no. 4, pp. 180–182.
10. Kuropatenko, V.F., Shestakovskaya, E.S., and Yakimova, M.N., 2016, Shock waves in a gas sphere, *Vestnik YuUrGU. Matematicheskoe modelirovanie i programmirovanie* (Bulletin of the South Ural State University. Ser. Mathematical Modeling and Programming), 2015, vol. 9, no. 1, pp 5–19.
11. Kuropatenko, V.F., Magazov, F.G., and Shestakovskaya E.S., The analytical solution of the problem of a convergent shock in the gas for one-dimensional case, *Vestnik YuUrGU. Matematika. Mekhanika. Fizika* (Bulletin of the South Ural State University. Ser. Mathematics. Mechanics. Physics), 2017, vol. 9, no. 4, pp. 52–58.
12. Kuropatenko, V.F., Magazov, F.G., and Shestakovskaya, E.S., Focusing cylindrically symmetric shock in a gas, in: *Proc. Intern. Conf. "XIII Zababakhin Scientific Talks,"* Snezhinsk: RFNC-RRITP, 2017, pp. 39–40.
13. Kuropatenko, V.F. and Shestakovskaya, E.S., Convergent shock in a gas for large values of a self-similar coefficient, in: *Proc. Intern. Conf. "XIII Zababakhin Scientific Talks,"* Snezhinsk: RFNC-RRITP, 2017, pp. 54–56.
14. Bogoyavlensky, O.I., *Metody kachestvennoy teorii dinamicheskikh sistem v astrofizike i gazovoy dinamike* (Methods of Qualitative Theory of Dynamical Systems in Astrophysics and Gasdynamics), Moscow: Nauka, 1980.

Translated by M. Lebedev